

# Implementation of an Anti-Windup Scheme for Vertical Controllability in the DIII-D Tokamak

Eugenio Schuster<sup>a</sup>, Michael L. Walker<sup>b</sup>, David A. Humphreys<sup>b</sup>, and Miroslav Krstic<sup>a</sup>

<sup>a</sup>*Mechanical and Aerospace Engineering, University of California at San Diego, La Jolla, CA 92093-0411*

<sup>b</sup>*General Atomics, PO Box 85608, San Diego, CA 92186-5608*

**Abstract.** An anti-windup compensator is designed for a given predesigned nominal plasma vertical position controller guaranteeing global vertical stabilization of the plasma in the presence of actuator saturation for all reference commands. The anti-windup synthesis problem is to find a nonlinear modification of the nominal controller that prevents vertical instability and undesirable oscillations but leaves the nominal closed loop unmodified when there is no input saturation. Design and performance simulations are complete. The different implementation stages, already in process, are described.

## I. INTRODUCTION

The Advanced Tokamak (AT) operating mode is the principal focus of the DIII-D tokamak. Demands for more varied shapes of the plasma and requirements for high performance regulation of the plasma boundary and internal profiles are the common denominator of the AT operating mode in DIII-D [1]. In order to be prepared for the higher control demands arising in AT scenarios, current efforts are focused on the development of an integrated multivariable controller [2] to take into account the highly coupled influences of equilibrium shape, profile, and stability control. The first step of this project is the design of the shape and vertical controller that will be integrated in the future with control of plasma profiles. The time-scale properties of the system allow the separation of the vertical stabilization problem, which is the focus of this paper, from the shape control problem.

The problem of vertical and shape control in tokamaks was and is still extensively studied in the fusion community. A recent summary of the existing work in the field can be found in [3]. Several solutions for the design of the nominal controller were proposed for different tokamaks using varied control techniques based on linearized models. However, only a few of them [4] take into account the control voltage constraint in the design of the nominal controller. The goal of this paper is not the design of the nominal controller but the design of an anti-windup compensator that blends any given nominal controller, which is designed to fulfill some local performance criterion, with a nonlinear feedback designed to guarantee stability in the presence of input saturation but not necessarily tuned for local performance.

The isoflux control method, now in routine use on DIII-D, exploits the capability of the real time EFIT plasma shape reconstruction algorithm to calculate magnetic flux at specified locations within the tokamak vacuum vessel. Fig. 1 illustrates a lower single null plasma which was controlled using isoflux control. Real time EFIT can calculate very

accurately the value of flux in the vicinity of the plasma boundary. Thus, the controlled parameters are the values of flux at prespecified control points along with the X-point  $r$  and  $z$  position. By requiring that the flux at each control point be equal to the same constant value, the control forces the same flux contour to pass through all of these control points. By choosing this constant value equal to the flux at the X-point, this flux contour must be the last closed flux surface or separatrix. The desired separatrix location is specified by selecting one of a large number of control points along each of several control segments. An X-point control grid is used to assist in calculating the X-point location by providing detailed flux and field information at a number of closely spaced points in the vicinity of the X-point.

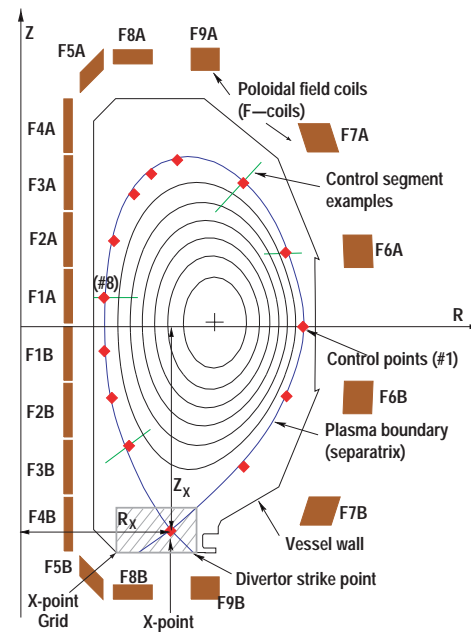


Fig. 1. Lower single null plasma. Isoflux control points and X point grid used for calculation of shape error.

Time-scale separation of vertical and shape control appears to be critical for DIII-D, since multivariable shape controllers can require significant computation. Fig. 2 shows the closed loop system comprised of the DIII-D inner plant and a stabilizing controller. This system is stable locally (when there is no input saturation) and the 6 coil currents F2A, F2B, F6A, F6B, F7A, and F7B are approximately controlled to a set of input reference values. The inner loop provides as input actuators the 6 vertical coil current reference signals, the centroid vertical position reference signal and up to 12 shape coil command voltages.

This method implemented for sharing actuators involves constructing a linear controller that simultaneously stabilizes and provides control of vertical coil currents on a fast time scale. By integrating control of the vertical control coils into a stabilizing controller, conflicts between shape and vertical control use of these coils is eliminated. “Frequency sharing” is accomplished explicitly with an H-infinity loop shaping design by weighting low frequencies to regulate the coil currents and high frequencies to stabilize the plasma. This technique ensures robust stability of the combined control.

To take into account the nonlinear nature of the power supplies we incorporate a full nonlinear model of them into an augmented saturation block as it is shown in Fig. 2 instead of using a linearized model of the choppers for the inner plant model. The nominal linear vertical controller can be synthesized using no information of the choppers and its output then represents directly the desired coil voltages. A chopper inverse function computes the necessary command voltages within the saturation levels to make the output voltage of the choppers equal to the desired coil voltages. When the chopper inverse function fails calculating those command voltages we have saturation. Although the saturation levels of the command voltages  $V_c$  are still fixed values ( $\pm 10V$ ), the saturation levels of the augmented saturation block are now functions of time (coil current and DC supply voltage  $V_{ps}$ ).

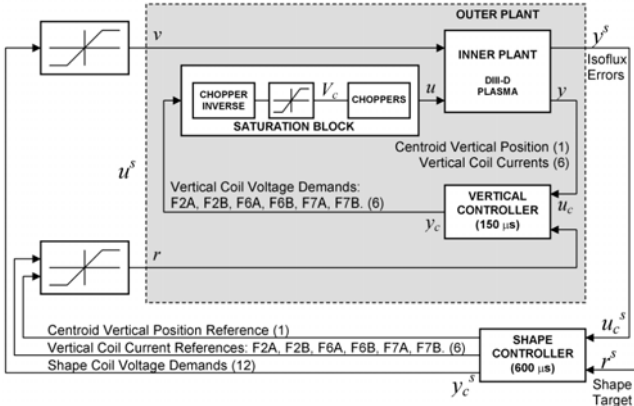


Fig. 2. Plant architecture.

In order to make this approach successful the inner controller (vertical controller) must guarantee the stability of the plant for all commands coming from the outer controller (shape controller). Due to the constrained control, the nominal linear vertical controller may fail to stabilize the vertical position of the plasma inside the tokamak when large or fast disturbances are present or when the references coming from the shape controller change suddenly. Although the saturation of coil currents and voltages is a common problem in tokamaks and there are efforts to minimize the control demand for shape and vertical control and to avoid saturation [5], [6], the saturation of the actuators are generally not taken into account in the design of the nominal controllers in present works. The inner loop design must take care then of the windup of the actuators of that loop and ensure vertical stability for any command coming from the outer controller.

The anti-windup synthesis problem is to find a nonlinear modification of the predesigned nominal linear controller that prevents vertical instability and undesirable oscillations but leaves the nominal closed loop unmodified when there is no input saturation.

Due to the characteristics of our problem we follow the ideas introduced in the companion papers [7], [8], and also discussed in [9] for exponentially unstable systems. This technique has been shown to be successful in several case studies. However, the method must be modified and complemented in order to fulfill the performance requirements of our system [10].

The paper is organized as follow. Section II introduces the characteristics of the plant. The basis of the anti-windup augmentation is presented in Section III. Section IV discusses the implementation steps. Some other considerations about robustness and computational effort are presented in Section V. Conclusions are presented in Section VI.

## II. PLANT STRUCTURE

Fig. 2 illustrates the architecture of the plant. The dynamics of the inner plant can be modeled as

$$\begin{bmatrix} \dot{x}_s \\ \dot{x}_u \end{bmatrix} = \begin{bmatrix} A_s & A_{su} \\ 0 & A_u \end{bmatrix} \begin{bmatrix} x_s \\ x_u \end{bmatrix} + \begin{bmatrix} B_s \\ B_u \end{bmatrix} u + \begin{bmatrix} E_s \\ E_u \end{bmatrix} v \quad (1)$$

$$y = Cx + Du + Gv \quad (2)$$

where the vector  $u$  of dimension  $m=6$  are the voltages of the vertical coils F2A, F2B, F6A, F6B, F7A and F7B, the vector  $v$  of dimension  $q=12$  are the voltages of the remaining shape coils, the vector  $y$  of dimension  $p=7$  consists of the six vertical coil currents and the plasma centroid position. Due to the composition of the output vector it is convenient to write the reference for the nominal controller as  $r=[r_I \ r_Z]^T$  where  $r_I$  are the current references for the six vertical coils and  $r_Z$  is the centroid position reference. We write the plant of our system in state-space form separating the stable modes  $x_s$  of dimension  $n_s$  from the exponentially unstable modes  $x_u$  of dimension  $n_u$  where the dimension of the state vector  $x$  is  $n=n_s+n_u$ . The eigenvalues of  $A_s$  have non-positive real part whereas the eigenvalues of  $A_u$  have positive real part. The main characteristics of our plant can be summarized as:

1. There is only one unstable eigenvalue, i.e.,  $n_u=1$ , and the  $n_s=n-1$  stable eigenvalues are strictly negative. However, some of them are very close to zero (slow modes).
2. The saturation of the channel  $i=1 \dots m$  of the controller is a function of time (coil load current and DC supply voltage).
3. There is no direct measurement of the unstable mode.
4. In addition to the vertical coil voltages  $u$ , we have the shape coil voltages  $v$  as an additional disturbance input of the inner plant.

In addition, we consider that a nominal controller with state  $x_c$  of dimension  $n_c$ , input  $u_c$  of dimension  $p$ , output  $y_c$  of dimension  $m$  and reference  $r$  of dimension  $p$ ,

$$\begin{aligned} \dot{x}_c &= f_c(x_c, u_c, r) \\ y &= h_c(x_c, u_c, r) \end{aligned} \quad (3)$$

has been previously designed so that the closed loop system with interconnection conditions  $u=y_c$ ,  $u_c=y$  is well-posed and internally stable. When the controller output is subject to saturation, i.e., the interconnection conditions are  $u=sat(y_c)$ ,  $u_c=y$ , the nominal controller cannot guarantee stability anymore.

### III. ANTI-WINDUP COMPENSATOR

Under the presence of saturation, the synthesis of an anti-windup scheme is necessary and the interconnection conditions are modified to  $u=sat(y_c+v_1)$ ,  $u_c=y+v_2$ , where  $v_1$  and  $v_2$  are the outputs of the anti-windup compensator [11]

$$\begin{aligned} \dot{x}_{aw} &= Ax_{aw} + B[sat(y_c + v_1) - y_c] - [1 - \gamma(y_c + v_1)]\delta x_{aw} \quad (4) \\ v_1 &= (\beta(x_u) - 1)y_c + K_u[x_u - \beta(x_u)(x_u - x_{awu})] \\ v_2 &= -Cx_{aw} - D[sat(y_c + v_1) - y_c] \end{aligned}$$

where  $\delta$  is a positive constant. The compensator state  $x_{aw}$  is also written separating stable  $x_{aws}$  and unstable modes  $x_{awu}$ .

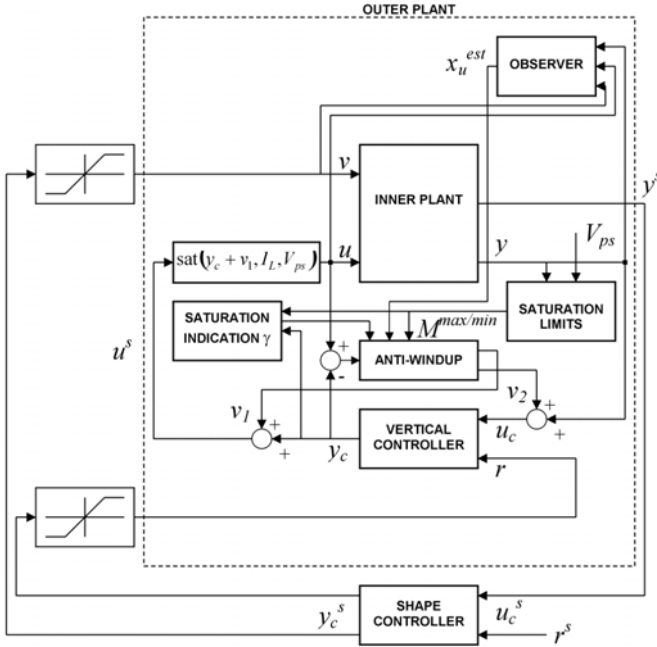


Fig. 3. Anti-windup augmentation for the inner-loop.

The anti-windup scheme is illustrated in Fig. 3. In addition to modifying the nominal controller when input saturation is encountered, the anti-windup compensator modifies the closed loop if the exponentially unstable modes get close to the boundary of some reasonably large subset of the region where these unstable modes are controllable with the given bound on the control. The signal  $\beta$  is defined as

$$\beta(x_u) = \begin{cases} 1, & x_u \in \mathcal{X}_{lower} \\ 0, & x_u \notin \mathcal{X}_{upper} \end{cases} \quad (5)$$

and interpolated in between, where  $\mathcal{X}_{lower} \subset \mathcal{X}_{upper}$  are subsets of  $\mathcal{X}$ , the domain of attraction of the disturbance-free system subject to the saturation of the output controller or what we

call controllable region. The freedom to define  $\mathcal{X}_{lower}$  and  $\mathcal{X}_{upper}$  is a tool the designer has to deal with the disturbances that although not modeled are present in the system as well as with any potential uncertainty in the determination of  $\mathcal{X}$ . The smaller  $\mathcal{X}_{lower}$  and  $\mathcal{X}_{upper}$ , the bigger the disturbances tolerated by the system without escaping the controllable region  $\mathcal{X}$ . The gain  $K_u$  is such that  $A_u + B_u K_u$  is Hurwitz. The function  $\gamma$  is an indication of saturation, being zero if none of the input channels is saturating and one otherwise. It is important to note at this point that this scheme requires the measurement or estimation of the exponentially unstable modes  $x_u$ .

### IV. IMPLEMENTATION STAGES

We describe in this section the different implementation stages already under way in the DIII-D tokamak.

#### A. Observer: Estimation of the unstable mode

A state observer is designed for the estimation of the unstable mode of the plant because a direct measurement is not available. It is important to realize that from the observer we only need to know if the unstable mode is inside  $\mathcal{X}_{lower}$  or outside  $\mathcal{X}_{upper}$ . An accurate estimation is not required to make the anti-windup compensator achieve its goals. In addition it is always possible to compensate the inaccuracy of the observer with a convenient selection of these two sets. But although the estimation does not need to be very accurate it must be fast and the observer must be designed accordingly. A high gain observer is required in this case to ensure that the estimation is fast enough to prevent any excursion of the unstable mode outside the controllable region. The anti-windup compensator (4) is implemented replacing  $x_u$  by  $x_u^{est}$ .

#### B. Saturation Limits - Controllable region computation

The computation of the controllable region  $\mathcal{X}$  requires two steps. In the first step we must estimate at each instant of time the saturation limits for the actuators. This is not straightforward because the output voltage  $V_o$  of the chopper power supplies are complicated nonlinear functions of an external power supply capacitor charging voltage  $V_{ps}$ , coil load current  $I_L$ , and command voltage input  $V_c$ , each of which also changes with time, i.e.,  $V_o = f(V_c(t), I_L(t), V_{ps}(t))$ . Based on the measurements of  $V_{ps}$  and  $I_L$ , and the limiting values for  $V_c$  ( $\pm 10V$ ), we can estimate the saturation limits  $M^{\min}(t)$  and  $M^{\max}(t)$  for  $V_o$ . In the second step we use the dynamics of the unstable mode in (1) and the saturation limits computed in the first step to compute the range of  $x_u$  for which we have control authority. This interval for  $x_u$  defines the controllable region

$$\mathcal{X} = \{x_u : x_u^{\min} < x_u < x_u^{\max}\} \quad (6)$$

#### C. Safeguard function $\beta$ in the anti-windup compensator

Once the controllable region  $\mathcal{X}$  is defined, the sets  $\mathcal{X}_{lower}$  and  $\mathcal{X}_{upper}$  are selected as subsets of it and the function  $\beta$  is implemented according to (5). The more conservative (smaller) the selection of  $\mathcal{X}_{lower}$  and  $\mathcal{X}_{upper}$ , the higher the tolerance of the system against uncertainties in the unstable mode estimation and the saturation limits (controllable region).

#### D. Saturation Indication $\gamma$

Ideally we have saturation when the input and output of the augmented saturation block in Fig. 2 are different. This is coincident with the moment when the command voltage  $V_c$  hits one of its limits ( $\pm 10V$ ). However, due to imperfect accuracy of the chopper model (chopper inverse function) we may have  $u$  different from  $y_c$  even without saturation of  $V_c$ . Therefore, we implement the saturation function  $\gamma$  based on the signal  $V_c$ . To avoid chattering we introduce a hysteresis loop, making  $\gamma=1$  when any of the channels reaches the limiting values ( $\pm 10V$ ) and making  $\gamma=0$  when all the channels return within a subset of  $[-10V, 10V]$ .

#### E. Chopper inverse function

The chopper inverse function allows us to gain accuracy avoiding the linearization of the chopper model, make the synthesis of the vertical controller simpler and more robust and simplify the design of the anti-windup compensator keeping the inner plant linear. A convergent iterative algorithm with low computational demand will be tested in this stage.

#### F. Anti-windup compensator

The last step is the implementation of the anti-windup compensator according to (4). The signal  $v_1$  is in charge of keeping the plant well-behaved whereas the signal  $v_2$  keeps the nominal controller well-behaved. The anti-windup compensator modifies the nominal loop through the signal  $v_1$  when the unstable mode (monitored by the function  $\beta$ ) is reaching the boundary of the controllable region ensuring stability of the plant. In addition, the nominal loop is modified by the anti-windup compensator through the signal  $v_2$  when the actuator saturates, hiding the saturation from the nominal controller and ensuring its good behavior.

### V. OTHER CONSIDERATIONS

The growth rate of the plant is directly related to the elongation of the plasma. The more elongated the plasma, the more unstable. This means that when we modify the shape of the plasma using the outer loop (shape controller), the plant of the inner loop is modified. However, the input-output relationship of the plant does not vary significantly when the growth rate varies. It is for this reason that the anti-windup compensator is very robust against changes in the growth rate. This same robustness is not exhibited by the observer because its operation is based on the state-space model and consequently on the growth rate  $A_u$ . According to the value of the growth rate  $A_u$ , which can be computed on-line, different models are used for the estimation of the unstable mode.

Due to the short time-scale of the inner loop the computational effort must be minimized. Although an observer scheduling is a must, simulation studies show that a very low order observer succeeds in giving an estimation of the unstable mode which is good enough to prevent the vertical instability of the plant. In addition a very low order (relative to the order of the plant) anti-windup compensator succeeds in providing the necessary input-output relationship even in the presence of uncertainties in the plant growth rate.

### VI. CONCLUSIONS

The proposed scheme has been shown in nonlinear simulations to be very effective in guaranteeing global stability of the inner loop in the presence of voltage saturation of the vertical coils. The scheme will be tested in experimental conditions and is being implemented in the Plasma Control System (PCS) at this moment. However, it is possible to anticipate at this stage the need and convenience of a conditioning of the signals coming from the shape controller. A watch-dog will monitor the additional input  $v$  and keep it from making the controllable region  $\chi$  shrink below a predesigned minimum size and from suddenly causing the unstable mode to be outside the controllable region. In addition, a rate limiter on  $r_1$  will be implemented to take into account the characteristic integration time of the coils.

The necessity of a similar anti-windup scheme for the outer loop is anticipated; not only due to the inherent limitations of its actuators but also due to the fact that the inner loop will modify, through the watch-dog and rate limiter, the control signals of the outer loop in order to preserve stability of the inner plant and improve performance. In this case we will deal with a stable (stabilized by the inner loop design) but nonlinear plant.

### REFERENCES

- [1] J. L. Luxon, "A design retrospective of the DIII-D tokamak", *Nuclear Fusion*, 42, pp. 614-33, 2002.
- [2] D. A. Humphreys, M. L. Walker, J. A. Leuer and J. R. Ferron, "Initial implementation of a multivariable plasma shape and position controller on the DIII-D tokamak," *Proceedings of the 2000 IEEE International Conference on Control Applications*, Anchorage, Alaska, USA, pp. 385-94, September 2000.
- [3] R. Albanese and G. Ambrosino, "Current, position and shape control of tokamak plasmas: A literature review," *Proceedings of the 2000 IEEE International Conference on Control Applications*, Anchorage, Alaska, USA, pp. 412-18, September 2000.
- [4] L. Scibile and B. Kouvaritakis, "A discrete adaptive near-time optimum control for the plasma vertical position in a tokamak," *IEEE Transactions on control systems technology*, Vol.9, no.1, p. 148, 2001.
- [5] G. Ambrosino, M. Ariola, A. Pironti, A. Portone and M. Walker, "A control scheme to deal with coil current saturation in a tokamak," *IEEE Transactions on control systems technology*, Vol.9, no.6, p. 831, 2001.
- [6] R. Albanese, G. Ambrosino, A. Pironti, R. Fressa and A. Portone, "Optimization of the power supply demand for plasma shape control in a tokamak," *IEEE Transactions on magnetics*, Vol.34, no.5, p. 3580, 1998.
- [7] A. R. Teel and N. Kapoor, "The  $L_2$  anti-windup problem: Its definition and solution," *Proceedings of the 4th ECC*, Brussels, Belgium, July 1997.
- [8] A. R. Teel and N. Kapoor, "Uniting local and global controllers," *Proceedings of the 4th ECC*, Brussels, Belgium, July 1997.
- [9] A. R. Teel, "Anti-Windup for Exponentially Unstable Linear Systems", *International Journal of Robust and Nonlinear*, vol.9, pp. 701-716, 1999.
- [10] E. Schuster and M. Krstic, "Refinement to Anti-Windup for Nonlinear Systems," submitted to the *2004 American Control Conference*, Boston, Massachusetts, USA, June 2004.
- [11] E. Schuster, M. L. Walker, D. A. Humphreys and M. Krstic, "Plasma Vertical Stabilization in Presence of Coil Voltage Saturation in the DIII-D Tokamak," *Proceedings of the 2003 American Control Conference*, Denver, Colorado, USA, June 2003.